Marine Environmental Research 220 (2026) 108180

Contents lists available at ScienceDirect

Marine Environmental Research

journal homepage: www.elsevier.com/locate/marenvrev

Preliminary evidence of intra-offshore wind farm variation in epibiotic assemblages from automated ROV image analysis

Joseph Marlow [a,b,*], John E. Halpin [a,b], Thomas A. Wilding [a,b]

[a] University of the Highlands and Islands, UHI House, Old Perth Road, Inverness, IV2 3JH, United Kingdom
[b] Scottish Association for Marine Science, Oban, PA37 1QA, United Kingdom

ARTICLE INFO

Keywords:
Biofouling
Machine-learning
Marine growth
Photogrammetry
ROV

ABSTRACT

As global energy demand grows, our oceans are becoming increasingly industrialised. In the North Sea, one of the world's most developed marine regions, offshore infrastructure is shifting from isolated hydrocarbon platforms to large multi-turbine offshore wind farms (OWFs). These structures support diverse epibiotic assemblages which can influence structural integrity, alter ecological processes, and affect ecosystem service provisioning (e.g. water filtration). While epibiotic assemblage composition and zonation is well characterised on solitary structures, little is known about this varies at the intra-OWF scale. Our study explores this variation using ROV footage from a UK OWF; the foundations of two jacketed turbines situated at both the edge and centre of the OWF footprint were surveyed across all legs and depths, and the cover of five dominant epibenthic taxa quantified using a combination of structure-from-motion photogrammetry and machine-learning-based taxonomic segmentation. Epibiotic assemblages were dominated by anemones (*Metridium senile*) at intermediate depths, with increasing abundance of other target taxa at greater depths. While depth was the primary structuring factor, assemblage composition also appeared to vary with cardinal orientation and turbine position, with higher coverage of most target taxa at the OWF centre (notably soft corals (*Alcyonium digitatum*)). These patterns may be influenced by turbine-induced changes in downstream turbulence, stratification, and resource availability. While a limited sample size, our results suggest intra-OWF epibiotic heterogeneity, implying assemblage structure varies beyond depth zonation. As offshore wind development accelerates, research is needed to determine this variability's extent and drivers, helping to manage the consequences of an industrialised seascape.

1. Introduction

Over 6000 offshore fixed and floating oil & gas (O&G) structures have been installed in the world's oceans, with a further 5000 wind turbines (34 GW) added to our seas in the last 30 years (Gourvenec et al., 2022). As the world's energy requirements continue to rise, and nations seek to improve their energy security, the demands on offshore energy developments have never been so high. In our efforts to avoid the worst effects of climate change, global society is also pursuing a net zero agenda, which means the nature of offshore energy is changing. If we are to avoid a 1.5 °C temperature rise, then global offshore wind capacity needs to reach almost 500 GW by 2030 (IRENA, 2023), requiring a dramatic increase in the number of offshore structures (~13,000) in the coming decade (McCoy et al., 2024).

Regardless of the energy source, all offshore developments require some form of infrastructure in the marine environment, the presence of which contributes to "ocean sprawl" (Duarte et al., 2013; Firth et al., 2016) and is recognised as having significant ecological impacts at local and regional scales (Coates et al., 2014; Harris et al., 2025; Perrow et al., 2011; Slavik et al., 2019). As hard substrates (steel or concrete) of varying complexity in what are often soft-sediment dominated environments, man-made structures (MMS) represent a substantial increase in available (artificial) hard-substrate habitat; in parts of the Gulf of Mexico it is estimated that MMS contribute nearly 30% of the regions reef habitat (Bull and Love, 2019). Acting as "de-facto" artificial reefs, the epibiotic flora and fauna which colonise these MMSs (collectively known as biofouling or "marine growth") can substantially add to (and surpass) local biodiversity and biomass (Coolen et al., 2020b; Friedlander et al., 2014; Krone et al., 2013). The marine growth also has the potential to affect the structure and function of the wider environment; e.g. influencing local primary productivity through extensive filter feeding communities (Krone et al., 2013), spillover of marine growth

* Corresponding author. University of the Highlands and Islands, UHI House, Old Perth Road, Inverness, IV2 3JH, United Kingdom.
E-mail address: joseph.marlow@uhi.ac.uk (J. Marlow).

https://doi.org/10.1016/j.marenvres.2026.108180
Received 5 March 2026; Received in revised form 2 June 2026; Accepted 3 June 2026
Available online 4 June 2026

species into the neighbouring environment (Wilhelmsson and Malm, 2008), or increased habitat provision and enrichment of adjacent sediment through detachment and deposition of turbine-associated biota and waste (Coates et al., 2014; Lefaible et al., 2023). At a regional scale, MMS can act as stepping stones, enhancing connectivity between disparate benthic communities (in both natural and artificial habitats) and expanding their distribution (including endangered (Henry et al., 2018; McLean et al., 2022) and non-native species (Kerckhof et al., 2011)) into regions where they were previously absent (Bishop et al., 2017; Molen et al., 2018; Sammarco et al., 2014).

In the North Sea, which is one of the most developed bodies of water on the planet, and one of the most researched (Lemasson et al., 2024; Squire et al., 2026), we arguably have a better understanding of the ecological effects of MMS installation than anywhere else in the world. When an MMS is introduced to the marine environment in the North Sea, colonisation by (macro) marine growth occurs within months (Kerckhof et al., 2010; Todd et al., 2021). While the initial community of pioneer species can be highly diverse (20-50 macrobenthic species), these early colonisers are soon succeeded by different, more competitive species, with an intermediate peak in species richness until a stable mature community comprised of fewer, depth-zonated, dominant species is eventually reached (Kerckhof et al., 2010; Lefaible et al., 2023). Shallow depths (surface-20 m) are covered by macroalgae and the mussel *Mytilus edulis*; at intermediate depths (20-60 m) the anemone *Metridium senile* dominates and the soft coral *Alcyonium digitatum* is common; and below 60 m the cold water coral *Desmophyllum pertusum* can form large reef structures (Whomersley and Picken, 2003; Gass and Roberts, 2006; Krone et al., 2013; Van Der Stap et al., 2016). The reported timeline for the succession process differ between studies (6-10 years; Kerckhof et al., 2019; Whomersley and Picken, 2003) and it has been argued this presents an oversimplification of the situation with no permanent stable community observed on one Belgian offshore wind farm (OWF) after 11 years of immersion (Zupan et al., 2023). The likelihood is that marine growth assemblage composition is not a simple linear successional process but rather a complex and dynamic one, subject to continual change over time, possibly with multiple stable communities (Oshurkov, 1992; Sutherland, 1974). Fluctuations could arise not only from increasing immersion period but also from interacting factors such as predation, parasitism, disease, storm disturbance, and the arrival of non-native species, all of can vary with depth. Broader-scale drivers, including climate change and shifts in regional productivity, could further influence community composition across multiple spatial and temporal scales.

The question of spatial scale is important, because as we transition from predominantly hydrocarbon extraction to renewable energy production, the nature and scale of MMSs is changing. Where once, installations were either solitary jackets or grouped in small clusters, now installations are networks encompassing potentially hundreds of turbine foundations spread over thousands of square kilometres (Burdon et al., 2018; Nieradzinska et al., 2016). Understandably, previous research on marine growth communities has tended to focus on single structures (mostly O&G platforms; e.g. Forteath et al., 1982) or multiple unconnected structures (e.g. Schutter et al., 2019). Where the monitoring of marine growth has been reported in OWF arrays, these tend to have low replication and do not explicitly account for spatial variation (Dubois et al., 2025; Karlsson et al., 2022). Rarely has there been a detailed comparison of how marine growth communities vary across the scale of a single large OWF, although Maar et al. (2009) documented significant differences in the abundance of *M. edulis* between adjacent turbines. Community composition could be expected to vary over the scale of an OWF given that most sessile marine growth fauna are filter feeders, and we know that vertical mixing is increased within OWFs, reducing stratification and potentially enhancing plankton growth (Floeter et al., 2017; Dorrell et al., 2022) – i.e. increasing food availability.

Understanding intra-OWF marine growth community dynamics is important, but the tools we use to assess and manage their ecological impact largely assume marine growth equivalency across all turbines. For instance, ecosystem models commonly used to assess the ecological effects of such developments (e.g. Ecopath with Ecosim, EwE) are often not designed to operate at fine spatial scales. They typically assume a uniform biomass per square metre for a given depth or habitat type across the OWF footprint within a broader ecosystem (e.g. Raoux et al., 2019, 2017). Even studies employing spatially explicit models that are capable of resolving intra-wind farm variation in marine growth biomass (e.g. Ecospace) rarely do so in practice, and often focus on a single taxa (e.g. Le Marchand et al., 2025).

Part of the problem is that the majority of our understanding of marine growth community dynamics comes from the analysis of industry video data collected using remotely operated vehicles (ROVs) as part of regular structural integrity inspections (e.g. Schutter et al., 2019; Thomson et al., 2018; Todd et al., 2020, 2021; Van Der Stap et al., 2016). These "free" data can be extensive but engineering priorities rather than ecological questions dictate ROV survey procedures; footage is often low resolution, often targeting specific components and rarely standardized across turbines or depths (see review by McLean et al., 2020). The resulting imagery provides poor spatial resolution for detecting subtle intra-wind farm variation in marine growth dynamics, and the poor or inconsistent image quality further complicates accurate taxonomic identification and quantitative analysis. Rather than repurposing GVI footage, McLean et al. (2020) suggest a better approach is to opportunistically use industry ROV "downtime" to conduct dedicated scientific surveys, and that ROVs can be augmented with higher definition cameras, even in stereopairs, to produce spatially referenced 3D models of marine growth using Structure from Motion (SfM) photogrammetry. Photogrammetric 3D models can be scaled and orientated, to derive the area (Palma et al., 2018) or volume (Marlow et al., 2024) of specific taxa, and workflow efficiency can be enhanced with machine-learning based automatic species identification (Marlow et al., 2024; Pierce et al., 2021).

In this study, we conducted preliminary ROV surveys as an exploratory assessment of intra-wind farm spatial heterogeneity in marine growth dynamics. Our objectives were to 1) conduct ROV surveys of wind turbines within a large North Sea OWF, targeting turbines at the edge and centre of the wind farm footprint, 2) use a combined machine learning and SfM photogrammetry approach to assess variation in the abundance of dominant and conspicuous marine growth taxa in relation to depth, turbine position and orientation, and 3) assess the ecological and environmental implications of any intra-wind farm variability.

2. Methods

The methods for this study are explained in the sections below and outlined in Fig. 1.

2.1. Study site and ROV data

ROV video data was provided by an anonymous renewable energy operator of an OWF in the northern region of the UK sector of the North Sea, located approximately 15 km offshore. The area is characterised by predominantly westerly–northwesterly winds, with storm events driving an energetic wave climate, where significant wave heights are typically ~1–2 m but can exceed ~5–7 m during storms. Currents (~0.3 – 0.8 m s^{-1}) are primarily driven by the semi-diurnal tidal regime (although exceeding this during storm surges) and generally flow along a SSW–NNE axis (and vice versa). Substrate types comprise a mixture of sand, gravelly sand and, to a lesser extent, sandy gravel, with periodic seabed disturbance driven by combined wave–current forcing. The water column is typical of the northern North Sea, exhibiting seasonal stratification (thermocline ~10 – 30 m in summer) but is well mixed in winter. The water temperature ranges from approximately 6 - 12 °C from winter to summer, with a 1 °C difference between the stratified layers.

The OWF was comprised of ~80 jacket-based turbines (average

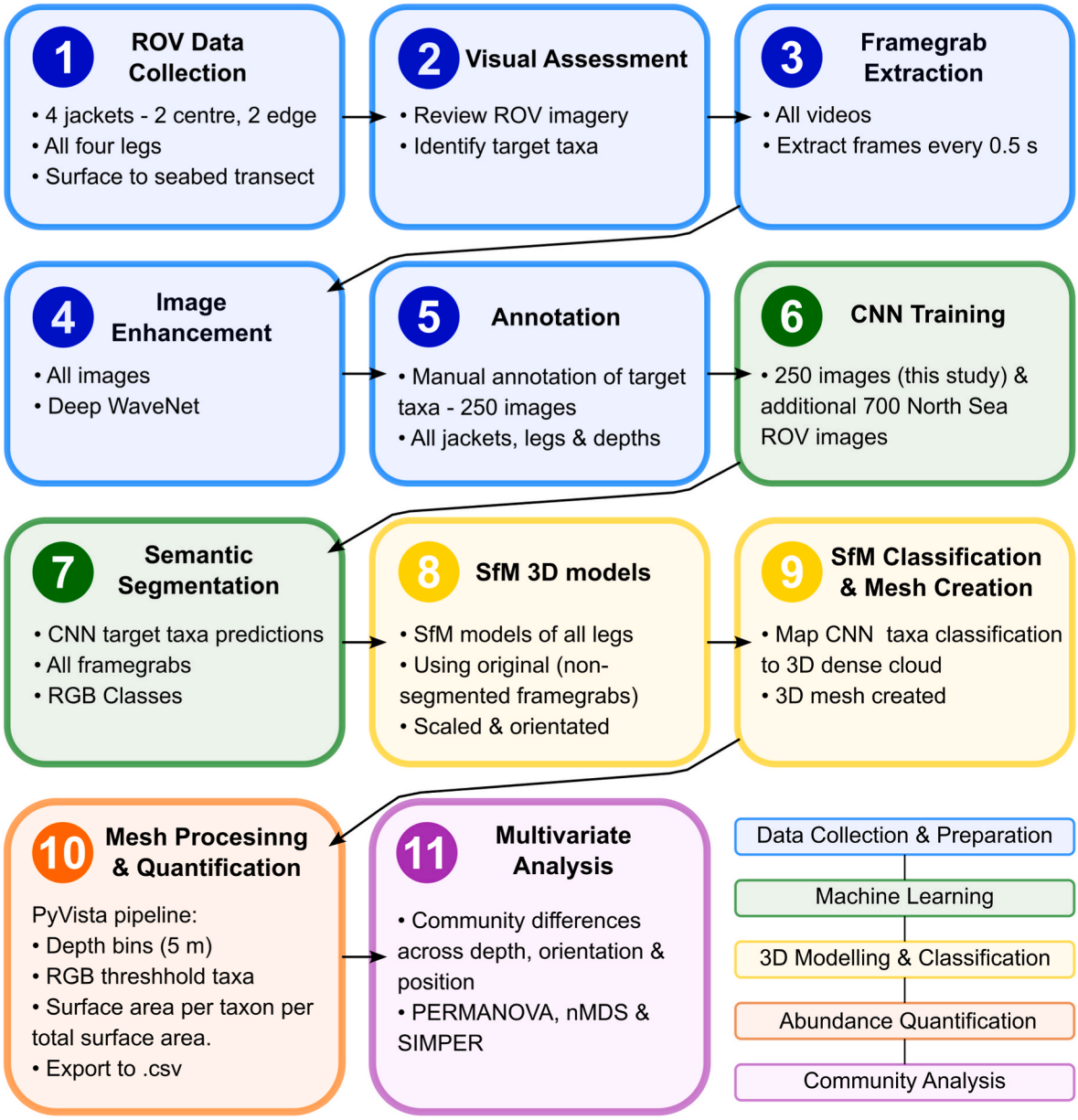

Fig. 1. Workflow for quantifying marine growth on OWF foundations in this study. Panels numbers represent sequential method steps and colours represent major workflow stages. (For interpretation of the references to colour in this figure legend, the reader is referred to the Web version of this article.)

depth ~35-40 m) of steel construction and approximately 1 m diameter. Each jacket had four legs with cardinal orientations of North-northeast (NNE), East-southeast (ESE), East-southeast (ESE), South-southwest (SSW) and West-northwest (WNW). Due to time restrictions, surveys were only conducted on four turbines, representing the wind farm edge (n = 2) and centre (n = 2), and at each jacket all four legs were surveyed. The structures had all been installed within a 16-week period in early autumn to early winter, and at the time of survey had been in place for between 3 years 6 months (edge) and 3 years 9 months (centre). Edge turbines were located along the southern and western margins of the array, whereas centre turbines were situated approximately 2.4–2.8 km and 5–6 km from the nearest and furthest array boundary respectively.

The data was obtained during ROV downtime during normal survey operations, following instructions from the authors. The ROV pilots were instructed to conduct a single pass down the outside of each leg, from the surface to the seabed, aiming for an average speed of ~0.1 m s^{-1}. The observation class ROV (Outland 2500, Outland Technology, Slidell, LA, USA) was equipped with laser scalers (20 cm separation) and a HD camera (GoPro™ Hero 8 camera, GoPro Inc., San Mateo, CA, USA) collecting video imagery with the camera set to 2.7k resolution, 60FPS, no image stabilisation, and "wide" lens setting.

2.2. Marine growth taxa

We conducted a preliminary visual assessment of the ROV imagery across all the structures to identify the target taxa for our study. This revealed that the most dominant and conspicuous species were the anemone *M. senile,* the soft coral *A. digitatum*, the hydroid *Tubularia indivisa,* the urchin *Echinus esculentus*, and the keel worm *Spirobranchus triqueter* (see example images in the Supplementary Material). These taxa are a commonly reported component of North Sea marine growth (e.g. Andersson et al., 2009; Van Der Stap et al., 2016; Zintzen et al., 2008a,b) and were the target taxa for our study and our machine learning model.

2.3. Machine-learning model

For each jacket leg video, framegrabs were extracted from the ROV video at 0.5-s intervals using Agisoft Metashape™. The objective was to segment these images by target taxa following the methods described in Marlow et al. (2024). However, our pre-existing convolutional neural network (CNN) had only been trained (700 images from a wide variety of North Sea ROV footage) on *A. digitatum, E. esculentus* and *M. senile,* and required additional training for *S. triqueter* and *T. indivisa.*

Additional training used 250 framegrabs selected to be representative of the entire dataset; across each of the jackets, jacket leg orientations and across all depths. During this process it was noted that many of the framegrabs exhibited colour distortion caused by light absorption and scattering, particularly at depth, which was exacerbated by insufficient lighting on the ROV at the time of capture. To avoid ambiguity caused by this distortion during image annotation, it was decided to aid the annotation process by enhancing all the ROV framegrabs prior to annotation, training and segmentation using the Deep WaveNet framework (Sharma et al., 2023), chosen for its high performance in underwater image restoration.

Following the additional training, all framegrabs from each jacket were segmented using a Mix Vision Transformer encoder (from SegFormer, Xie et al., 2021) combined with a simple U-net decoder (see Marlow et al. (2024) for more information), implemented using PyTorch Segmentation Models (Iakubovskii, 2019). The segmentation assigned a unique RGB colour value to each of the identified target taxa.

2.4. Photogrammetric model creation

SfM photogrammetric 3D models of each jacket leg were made in the software Agisoft Metashape™. The original, non-segmented framegrabs were used for image alignment and dense cloud creation steps (as per Marlow et al., 2024). Scaling was achieved by manually applying targets to the laser scaler points in the images and creating scale bars; a minimum of four scale bars equally placed along the length of the jacket, with a minimum acceptable total error of 5 mm. The dense cloud was correctly orientated by adding three targets to the seabed at the base of each jacket leg with known x,y and z distances. Prior to mesh creation, the dense cloud was classified (as per Pierce et al., 2021) by marine growth taxa using machine-learning based RGB classified semantic segmentation of the original ROV imagery.

2.5. Measuring taxa-specific abundance

Meshes for each of the jacket legs were manually trimmed within Agisoft Metashape™ to remove any components that were not explicitly part of the leg structure (e.g. seabed, vertical diagonal members, export cables). Meshes were then exported as individual ply. files into a custom python batch processing pipeline built using PyVista (Sullivan and Kaszynski, 2019), a 3D plotting and mesh analysis interface for the Visualization Toolkit (VTK). The pipeline consisted of the following three steps, 1) cropping of the mesh by 5 m depth intervals (6 intervals across 10-40 m depth), 2) segmenting the mesh with an RGB colour threshold to isolate each taxon, before 3) measuring the surface area of the resulting mesh/taxa and exporting values to.csv. The abundance of each taxon was subsequently measured as the surface area of each taxon as a function of the total mesh surface area for each 5 m depth interval. This taxa abundance by depth & jacket-leg matrix formed our key output and was used as the basis for subsequent multivariate analysis.

2.6. Statistical analysis

Abundance data was assessed in terms of assemblage compositional differences across depth (5 m depth bands), aspect (cardinal orientation of turbine legs) and position within the wind farm (centre vs edge). All data analyses were performed in R v4.4.1 within the interface Rstudio v2024.04.2.

To assess differences in benthic assemblage composition, a permutational multivariate analysis of variance (PERMANOVA) was conducted using the *adonis2()* function from the *vegan* package. Species abundance data were fourth-root transformed to down-weight the influence of highly dominant taxa and Bray–Curtis dissimilarity was used as the distance measure. To account for potential non-independence of abundance data from the same jacket, permutations were stratified by jacket, treating "Jacket ID" as a random blocking factor. Each term in the model was assessed independently using marginal sums of squares (by = "margin"), analogous to Type III or 'partial' sums of squares tests (Oksanen et al., 2025). The analysis tested for the effects of depth and aspect, but position (centre vs edge of the wind farm) was not included in the model due to its confounding with "Jacket ID"; with only four turbines (two per position category), there was insufficient replication to independently assess this effect within the stratified design.

To visualise patterns in assemblage composition, non-metric multidimensional scaling (nMDS) was performed using Bray–Curtis dissimilarity and the *metaMDS()* function from the *vegan* package. This ordination approach was selected due to its flexibility in handling non-linear relationships and high-dimensional ecological data. Ordination plots were labelled by position (edge vs centre) and included 2D bubble plots of individual species abundance to explore potential spatial patterns not included in the main PERMANOVA model.

To further examine which taxa contributed to compositional differences between depths, aspect and position, Similarity Percentage (SIMPER) analyses were conducted using the *simper()* function. Although position was not included in the main PERMANOVA model (due to confounding with the blocking structure (Jacket ID)), if the nMDS suggested an effect of position, the SIMPER was used in an exploratory capacity to identify species contributing most to observed dissimilarities between these groups.

3. Results

3.1. Models

The video allowed for good photogrammetric representation of the jacket legs with high proportion of images aligned across all structures (mean 72.7% ± 3.9 SE). The overwhelming majority image alignment failure was in the shallowest regions of the structures (0 - 10 m), and the models failed to reconstruct these regions. This was anticipated as these regions were dominated by highly mobile macroalgae (primarily *Laminaria hyperborea*, *Alaria esculenta* and rhodophyte turf, J. Marlow pers. Obs) which are known to create problems in image alignment (Spyksma et al., 2022). There was also concern that image alignment would fail in the deeper regions of the structures (due to the poor ROV illumination), but all models showed good alignment even in these areas.

3.2. Machine learning

The Segformer model performed well on the dataset, demonstrating a high Intersection over Union (IoU) score of 0.86 and accuracy of 0.98, with performance by taxa summarised in the confusion matrix in Fig. 2. For all taxa, the most common misclassification was a false negative; the taxon being missed and segmented as background (or no marine growth), suggesting an underestimate for all taxa. There were inter-taxa differences in the model performance; the worst performing class was *T. indivisa,* followed by *S. triqueter* (Fig. 2). Examples of the combination of photogrammetric and machine learning processes can be seen in Figs. 3 and 4.

3.3. Benthic assemblage composition

The epibiotic assemblage was dominated by the anemone *M. senile,* which across all structures and depths had a mean percentage cover of

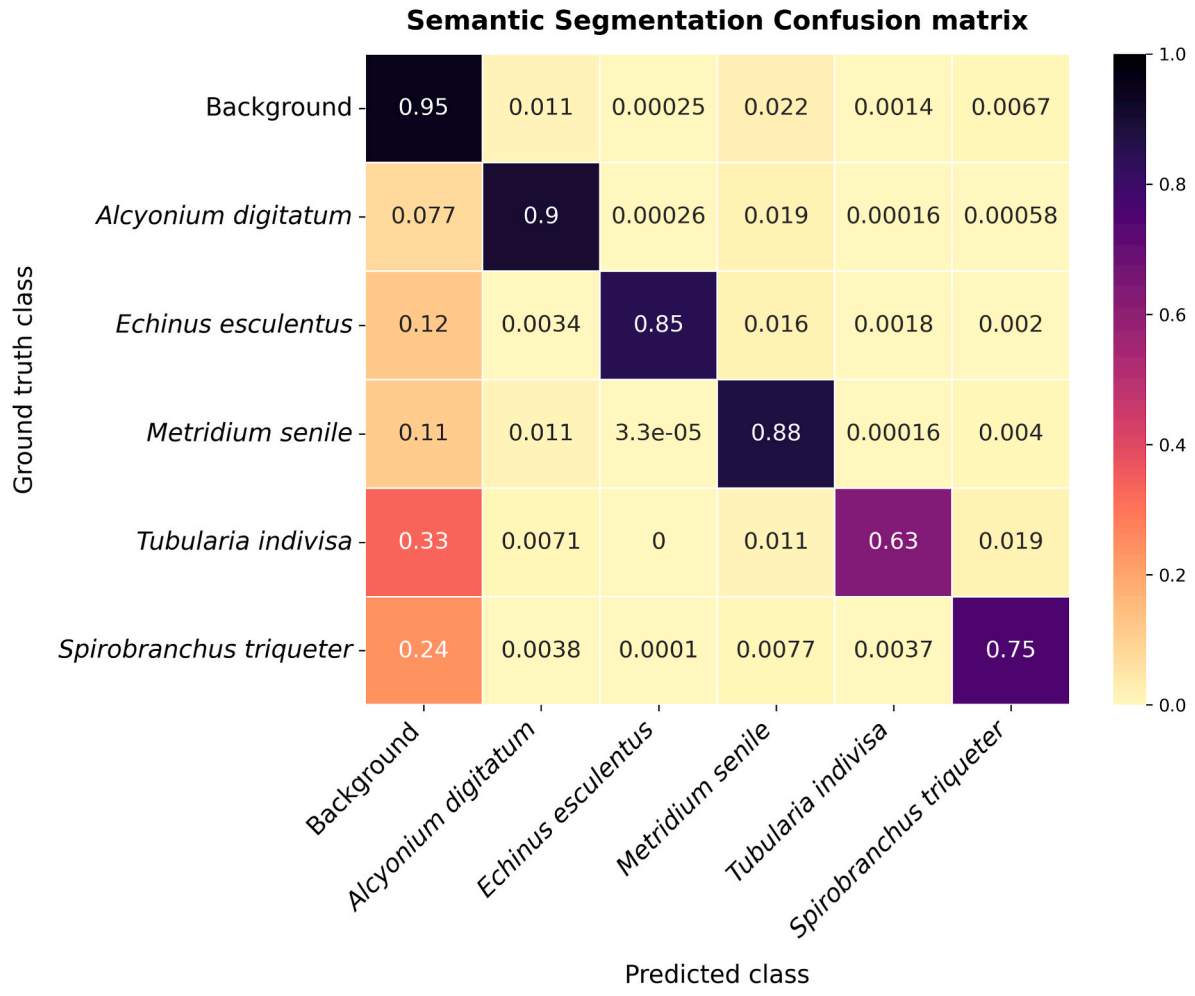

Fig. 2. Confusion matrix from SegFormer Backbone/U-Net on test data.

48% (±3.3 SE). This was followed by *S. triqueter* (6.9 ± 1.1% SE), *A. digitatum* (5.1 ± 0.80% SE), *T. indivisa* (1.3 ± 0.43% SE) and *E. esculentus* (0.10 ± 0.032% SE). On average, 33% (±2.4 SE) of the epibiota was labelled as unidentified.

Depth had a strong and significant effect on assemblage composition (PERMANOVA, $F = 22.754$, $R^2 = 0.547$, $p = 0.001$). The SIMPER analysis showed that the greatest depth-based dissimilarity (55.7%) was between the shallowest (10-15 m) and deepest (35-40 m) regions, with all target taxa exhibiting significantly different abundances (Supplementary Material). *M. senile* dominated from 10 to 25m but subsequently reduced in abundance at greater depths, concurrent with increases in the abundance of all other species, particularly *A. digitatum* and *S. triqueter* (Fig. 5).

Aspect had a significant but moderately weak effect on assemblage composition (PERMANOVA, $F = 2.4$, $R^2 = 0.035$, $p = 0.017$). The SIMPER analysis revealed a mean dissimilarity of 31-33% between aspects, driven mostly by differences in the cover of *A. digitatum* and *S. triqueter*, but most species contributions were not statistically significant ($p > 0.05$), suggesting that differences between aspects are subtle (Supplementary Material). The only significant differences were associated with a relatively high cover of *T. indivisa* on the ESE facing jacket legs (4 ± 4% SE); significantly higher than on SSW (0.7 ± 0.8% SE, $p = 0.022$) and WNW facing legs (0.5 ± 0.2% SE, $p = 0.046$), and although also higher than on the NNE facing legs (0.5 ± 0.8% SE), this was not statistically significant ($p = 0.070$). A low abundance of keel worm *S. triqueter* on WNW facing jackets legs also contributed to the aspect-based differences in assemblage composition, although the SIMPER analysis showed that this was only significant ($p = 0.032$) in relation to the NNE facing legs.

The NMDS plots (Figs. 6 and 7) indicated a large divergence in assemblage composition between turbines at the edge and centre of the wind farm, particularly at depths greater than 25 m. This was supported by the SIMPER analysis (Supplementary Material) which showed an overall 35.5% dissimilarity in assemblage composition between centre and edge communities; the percentage cover of all taxa, bar *M. senile,* was higher at the centre than the edge of the wind farm (*M. senile* showed a slight abundance decrease). The SIMPER analysis indicated that *A. digitatum* had the greatest impact on the positional dissimilarity (32% contribution; mean cover of 11 ± 9.5% SE at the centre vs 0.18 ± 0.33% SE at the edge ~ 5800% increase), followed by *S. triqueter* (24% contribution; mean cover of 10 ± 15% SE at the centre vs 3.4 ± 5.3% SE at the edge ~ 200% increase). While variation in *E. esculentus* contributed only 8% to positional dissimilarity due to its relatively low abundance on both centre and edge turbines, the urchin was over 470% more abundant on the former (0.074 ± 0.12% SE vs 0.013 ± 0.13% SE).

4. Discussion

Our study is, to our knowledge, the first to apply a combination of machine learning and SfM photogrammetry to industry ROV footage of marine growth, although these techniques have previously been used in isolation (machine learning: Gormley et al., 2018; Signor et al., 2023; SfM photogrammetry: Bayley et al., 2024). The combination provides an efficient method to visualise and quantitatively assess assemblage composition at ecologically and structurally relevant spatial scales. Like

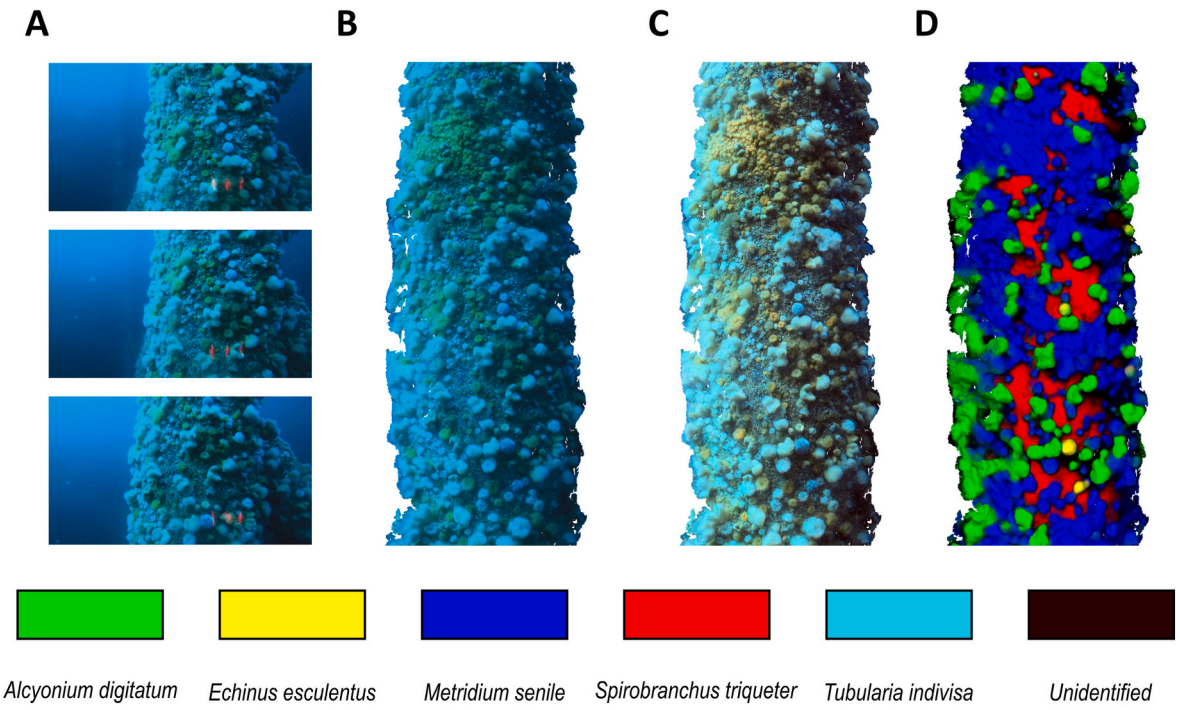

Fig. 3. Photogrammetry and automated taxonomic annotations workflow; original ROV framegrabs (A) textured mesh using original ROV imagery (B), enhanced imagery textured mesh (C) and mesh annotated by machine learning taxa (D).

all image-analysis, our automated taxonomic identification was constrained by what is visible in ROV imagery and by the training data. Consequently small or cryptic marine growth taxa (e.g. *Jassa herdmani*), which can be both abundant and diverse (Coolen et al., 2020b), were too small to be reliably detected and not included in our analysis. Nevertheless, our target taxa accounted for the majority of the spatial coverage on the structures and overall, our AI model performed very well in their detection. Where there was uncertainty, this was reflected in the regions that are segmented black in the 3D models and the higher proportion of false negatives for *T. indivisa* and *S. triqueter* in the confusion matrix. These particular taxa were minority classes in the training data and also restricted to the deeper regions of the structures, where the poorly illuminated footage showed the most colour distortion and image degradation. Human annotation was challenging in these regions, despite our enhancements, so similar difficulties in model performance were expected. In contrast, segmentation failures in the shallowest portions of the jackets were largely due highly mobile macroalgae, which is known to hinder image alignment (Spyksma et al., 2022), and deliberately not included in our training.

Dedicated marine growth surveys are prohibitively expensive and logistically challenging for scientific research and ecological monitoring, especially across large spatial scales. Consequently, most studies rely on industry GVI footage as a more accessible data source, and while this data may be free and extensive, the limitations and biases are numerous and well documented (McLean et al., 2020). Here we used an intermediate approach, using ROV "down-time" to conduct dedicated photogrammetric surveys and augmenting standard ROV equipment with high-definition cameras and laser-scalers. The resulting footage was of sufficient quality to produce high fidelity scaled 3D models of the marine growth, and to enable our machine-learning pipeline to produce accurate coverage estimates of our target taxa. However, while the surveys were conducted according to our guidance, we were not on site to review the data nor adapt methods and priorities in real time. The lack of oversite contributed to the inadequate illumination and insufficient spatial replication across the wind farm array. While this directed but remote approach is clearly an improvement over passively receiving GVI data, it remains a poor substitute for real-time survey supervision (whether remote or in-person), which we recommend whenever feasible.

Depth was the most important determinant of assemblage composition, consistent with observations from other North Sea OWFs (Coolen et al., 2020b; De Mesel et al., 2015; Krone et al., 2013). The upper sections of MMS are often characterised by intertidal taxa and macroalgal dominance (Karlsson et al., 2022), which is considered an important impact of MMS expansion within the North Sea, where intertidal substrates are largely absent from the offshore environment (Kerckhof et al., 2011). Although quantitative sampling of this zone was not possible in our study, macroalgae was observed to be dominant but notably, the mussel *Mytilus edulis* was absent, despite being a frequent and often highly abundant shallow species on other North Sea structures (20-30,000 individuals m^{-2}; Coolen et al., 2020a; Joschko et al., 2008). This absence may reflect local constraints such as limited larval supply (Coolen et al., 2020a; Forteath et al., 1982), insufficient water movement or predation pressure (Langhamer, 2010), illustrating how site-specific factors can effect assemblage composition within otherwise comparable depth zones. Below the macroalgal zone, *M. senile* was universally dominant across all structures to 25 m depth, consistent with other relevant studies (Coolen et al., 2020b; Karlsson et al., 2022). The species is known to be highly competitive and is thought to impede the survival of neighbouring recruits by smothering them with its pedal disk (Nelson and Craig, 2011). Below 25 m, *M. senile* abundance declined, and a more diverse assemblage was present, with higher abundances of all other target species. This pattern supports the negative relationship between *M. senile* dominance and species richness reported by Coolen et al. (2020b) and aligns with higher diversity observed near the seabed on other structures (Spielmann et al., 2023). Whomersley and Picken (2003) postulated that depth zonation is the product of both physical and biological mechanisms; shallow depths are structured by disturbance (waves) and light availability, intermediate depths by competition for food and space, and near-bottom communities by scour and sediment re-suspension. The evidence from our study broadly agrees with this analysis, but the absence of common taxa such as *M. edulis* demonstrates that taxonomic composition and dominance patterns within individual depth bands can vary substantially between studies.

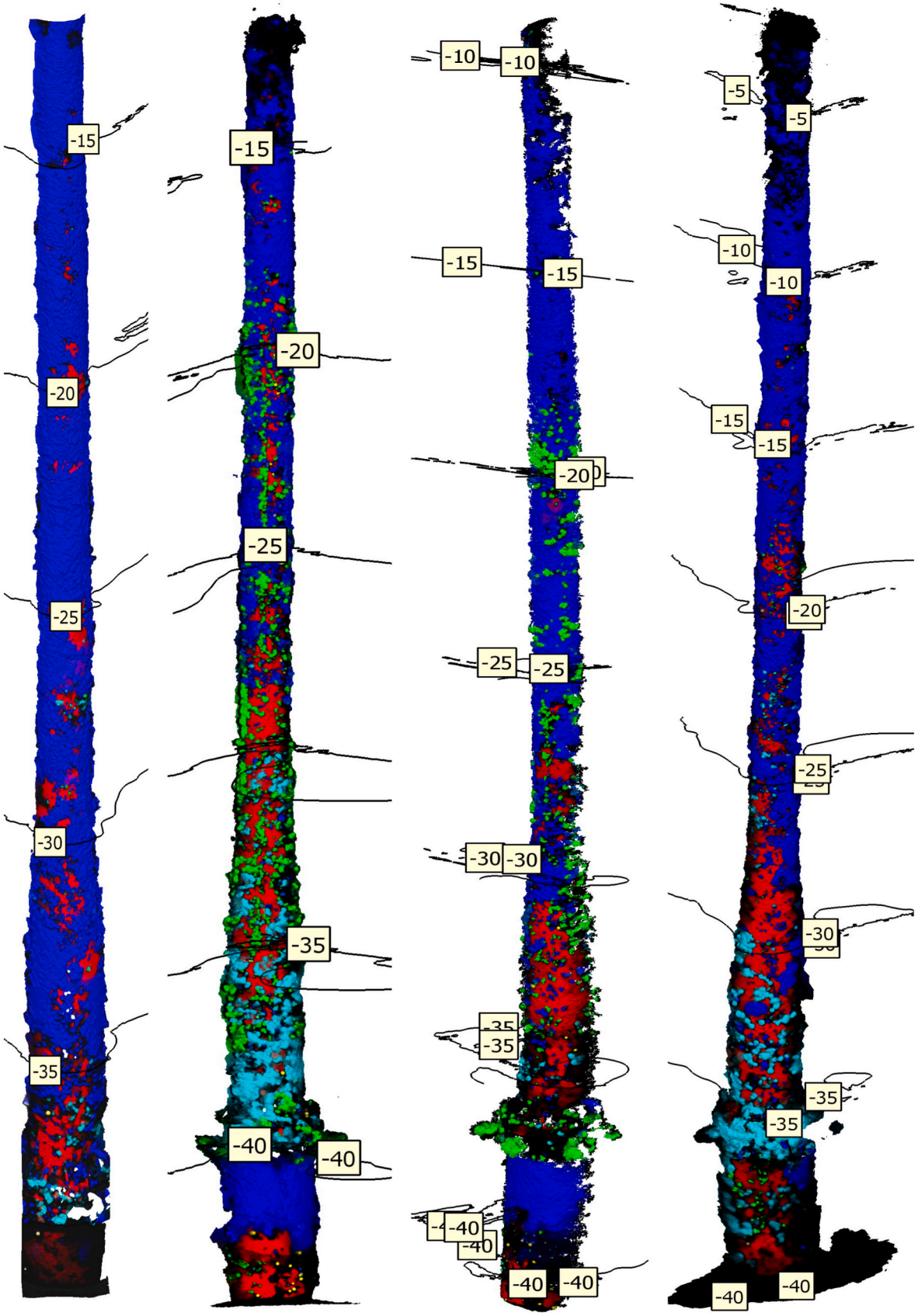

Fig. 4. Photogrammetric 3D models with automated taxonomic annotations (colours as per Fig. 3). Images are examples of annotated meshes of one leg (East-southeast) from each of the jackets; outer two are edge jackets and inner two are centre jackets. Depth contours are shown but note different maximum and minimum depths. (For interpretation of the references to colour in this figure legend, the reader is referred to the Web version of this article.)

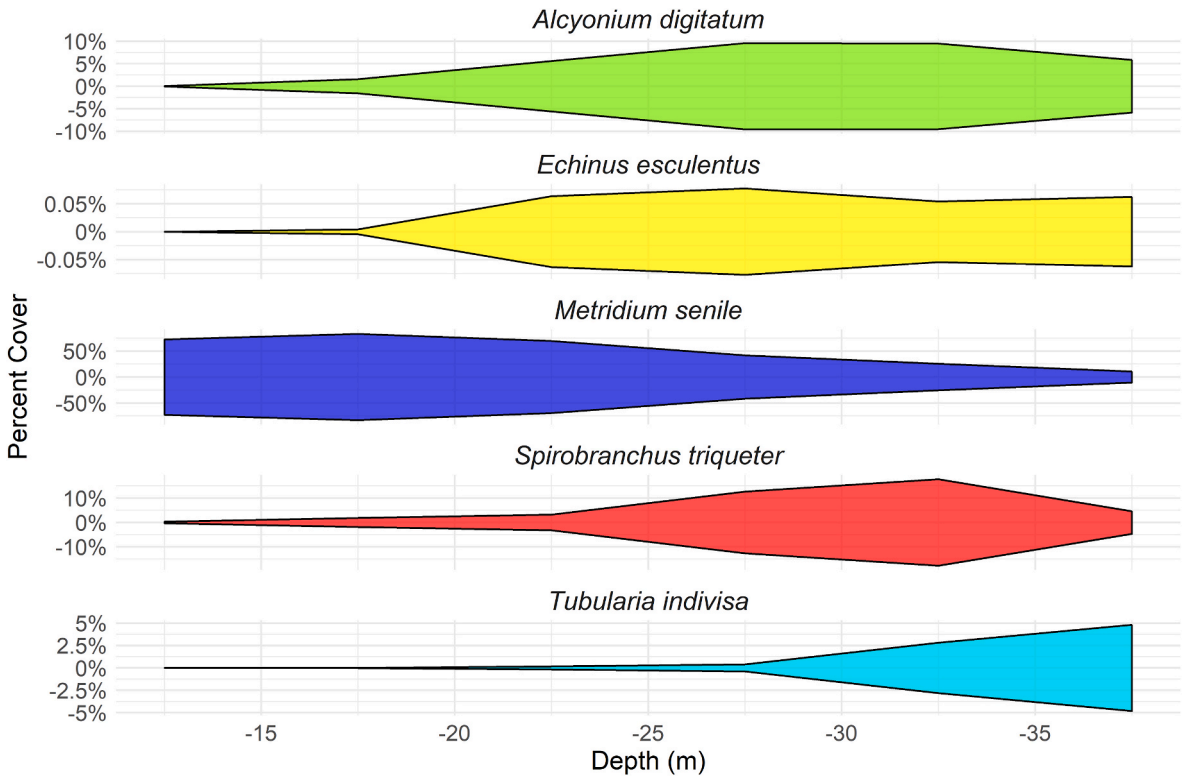

Fig. 5. Kite diagram of abundance (% cover) of target species across depth (10-40 m) across all structures. Note abundance scales specific to each taxa.

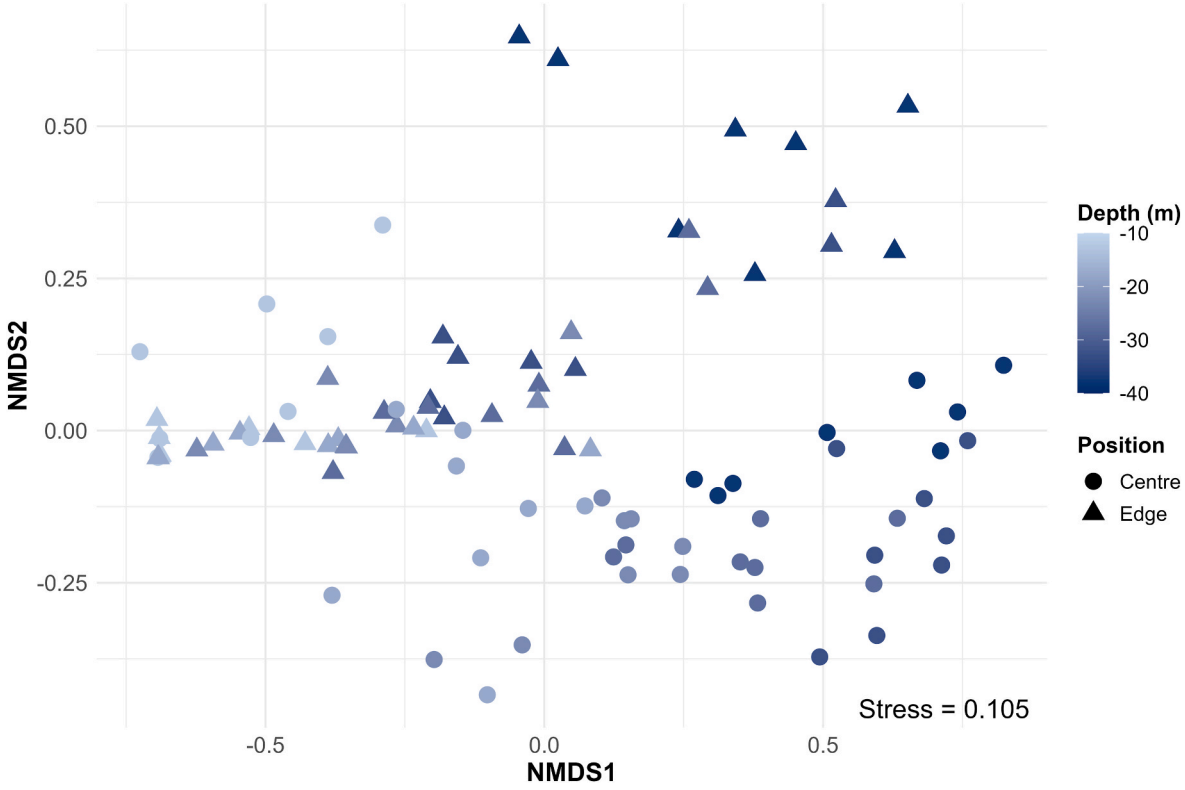

Fig. 6. Non-metric multidimensional scaling (NMDS) plot of wind farm marine growth assemblage composition. Differences in colour tone indicate different survey depths and data point shape show the relative position of turbine within the wind farm footprint. The 2-D NMDS solution had a stress of 0.104. (For interpretation of the references to colour in this figure legend, the reader is referred to the Web version of this article.)

Consequently, depth zonation on MMS is broadly comparable across the North Sea, but not sufficiently uniform to justify extrapolation between sites without local validation.

The cardinal orientation of subtidal surfaces might be expected to

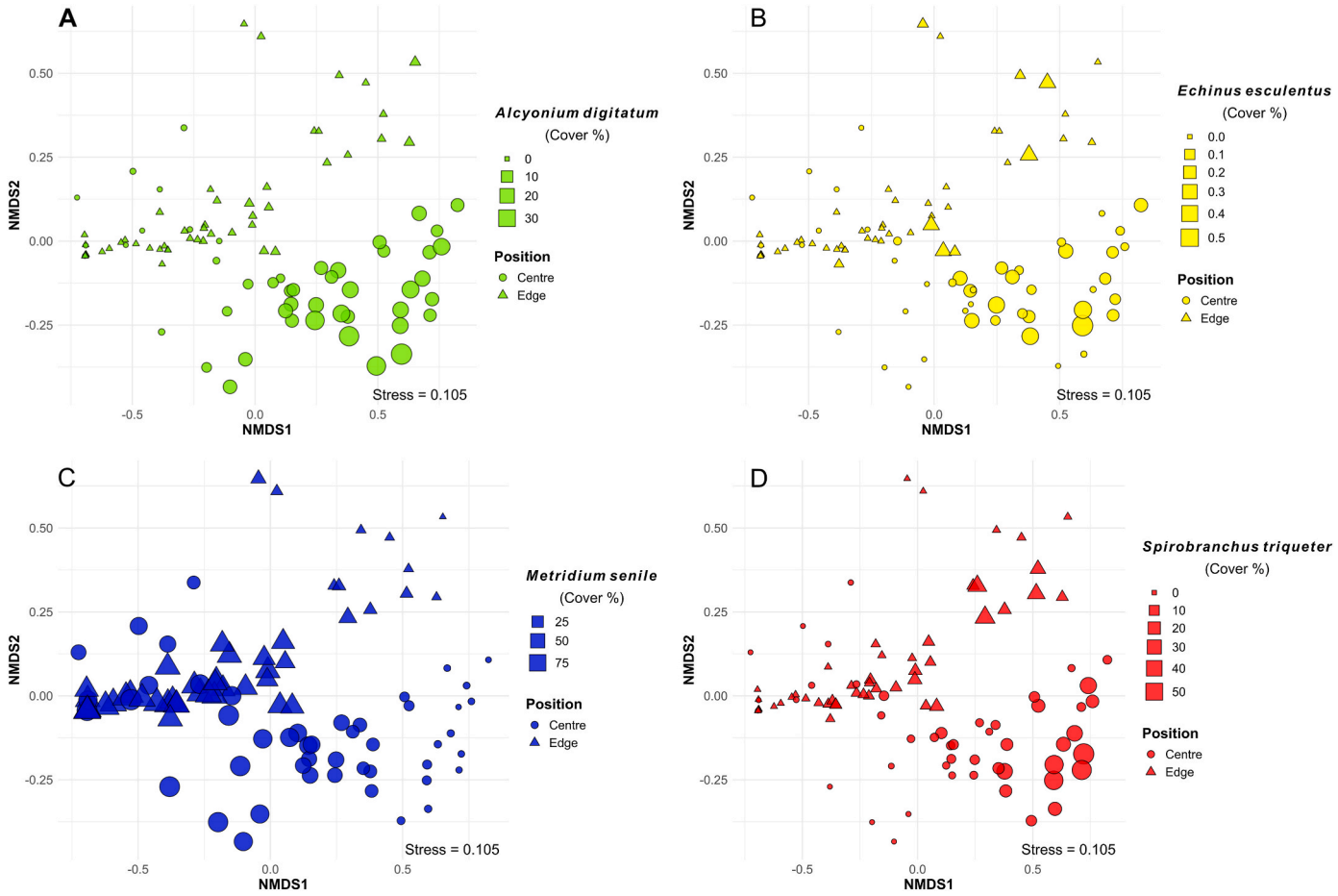

Fig. 7. *Non-metric multidimensional scaling (NMDS) plot of wind farm marine growth assemblage composition. Points represent 5m survey sections of each leg and are categorised by wind farm position. Overlapping 2D bubble size represents percentage cover of A) A.* digitatum, *B) E. esculentus, C) M. senile and D) S. triqueter.*

have some influence on assemblage composition through exposure to differing hydrodynamics, light and (consequently) temperature. However this has rarely been documented in subtidal communities (e.g. Angiolillo et al., 2016; Martins et al., 2013). In the context of marine growth, no studies to our knowledge have directly examined how cardinal orientation shapes assemblage composition on MMS, although jacket interior vs exterior differences have been reported (Guerin, 2009). In this study, some of the aspect-related variation was associated with the hydroid *T. indivisa* which was particularly abundant on east-southeast facing jacket legs. The hydroid is recognised as an early coloniser of bare substrates (Hiscock et al., 2010; Zintzen et al., 2008a, 2008b) but can also be seasonally dominant on high flow reefs in the Northeast Atlantic (Stamp et al., 2023). According to the principle of flow over bluff bodies, aspects perpendicular to the direction of current (i.e. ESE and WNW at our study site) would experience the greatest flow acceleration. While high abundance on the ESE aspect is therefore consistent with a high flow preference, the absence of a similar pattern on the WNW side remains unexplained.

Low replication meant that we could not generate precise parameter estimates for the effect of a turbines position within the wind farm footprint. However, our observations are commensurate with depth-driven transitions in species composition being influenced by spatial position. Although *M. senile* remained the dominant taxon at intermediate depths, deeper zones revealed divergent assemblage trajectories: conditions at the wind farm edge seem to promote continued *M. senile* dominance with increasing *S. triqueter* coverage, while central locations favour assemblages where *A. digitatum* and *S. triqueter* become dominant, accompanied by relatively greater numbers of *E. esculentus* and *T. indivisa*. Dominance by *M. senile* is typically associated with later successional stages (~4 years) in marine growth communities, whereas earlier stages are characterised by hydroids and tube worms (Whomersley and Picken, 2003). Higher abundances of these pioneer taxa on central structures could therefore indicate differences in successional stage; however, as central jackets were installed earlier (early autumn) than edge jackets (early winter), the opposite pattern would be expected if succession alone were driving the observed differences. Nevertheless, the timing of installation can be crucial as larval supply is highly seasonal (Want et al., 2017), with peak spawning in late summer for *M. senile* and in early winter for *A. digitatum* (Hartnoll, 1975; Lombardi and Lesser, 2010), with a similar larval duration for both species (~200 days; Molen et al., 2018). Consequently, the assemblage differences in later years could reflect differing larval availability at the time of installation or subsequent months. Alternatively, turbine positioning may directly influence assemblage composition by modifying local water column properties through enhanced downstream turbulence and mixing (Christiansen et al., 2023; Schultze et al., 2020). These changes could affect marine growth assemblage composition by affecting larval settlement or food availability through changes in flux or water column stratification. The latter mechanism remains poorly understood, with evidence suggesting that offshore turbines could both strengthen or weaken local stratification depending on background conditions and tidal–wind interactions (Daewel et al., 2022; Floeter et al., 2017). These effects, in turn, influence primary production and zooplankton abundance, altering the depth and intensity of the subsurface chlorophyll maximum. This may be particularly important when explaining intra-wind farm differences in assemblage zonation, given the majority of the dominant epibiota are suspension feeders. Moreover, the high abundance of these suspension feeding taxa could further shape

downstream (internal wind farm) communities through the depletion of available food sources, as has been observed inside mussel farms where phytoplankton and zooplankton concentrations can decline by up to 80% relative to ambient conditions (Maar et al., 2009; Petersen et al., 2008). This may be particularly relevant for *M. senile*, which is a selective filter feeder with a zooplankton diet that differs markedly from soft corals (*Alcyonium siderium*; Sebens and Koehl (1984)). Preferential removal of specific zooplankton prey by dense upstream *M. senile* communities could generate downstream conditions that are unsuitable for conspecifics but remain unaffected (or even advantageous) for competitors such as *A. digitatum*, facilitating a shift in dominance at the centre of the OWF.

Although exploratory, the observed spatial variability in dominant taxa may have important ecological and engineering implications if representative of wider OWF systems. From an ecological perspective, differences in the relative abundance of suspension-feeding organisms could influence local ecosystem functioning and ecosystem service provisioning, particularly through variation in water filtration rates, nutrient cycling and secondary habitat provision. For example, suspension feeding on turbines dominated by dense mussel aggregations are likely to have differing effects on the adjacent water column than those dominated by anemones or soft corals, through both different filtration efficiencies and prey selectivity. This may also influence the rate and composition of faeces and pseudofaeces deposition to the adjacent benthos, with potential consequences for benthic–pelagic coupling and local benthic community composition. These effects could be compounded by contrasting effects of epibenthic mortality (turbine drop-offs), with hard-bodied taxa such as mussels providing important secondary habitat (Lefaible et al., 2023), especially in soft sediment areas lacking scour protection. From an engineering perspective, spatial heterogeneity in biofouling composition may result in uneven distributions of biomass and hydrodynamic drag across structures, as different marine growth taxa are known to have differing densities and maximum thickness (Dubois et al., 2025; Marlow et al., 2024). This is particularly relevant for floating OWFs dynamic cable systems, which may be more sensitive to additional loading and changes in flow-induced forces than fixed-bottom infrastructure, and have additional concerns related to thermal insulation by marine growth (Maksassi et al., 2022, 2024). Consequently, improved understanding of fine-scale variability in marine growth could support more accurate cable design, maintenance planning, and ecological monitoring strategies.

Our exploratory study was inherently constrained by a focus on five conspicuous (but spatially dominant) taxa and limited turbine replication. As such it's important to acknowledge that our data only represents a subset of the full epibiotic assemblage and our observations of spatial heterogeneity should be interpreted with caution. Nevertheless, if the observed patterns are more widespread, these fine-scale spatial dynamics are currently underrepresented in ecosystem modelling and post-construction monitoring, despite consequential implications for both structural integrity and local ecological processes. As offshore wind developments continue to expand, determining the extent, driver and impact of intra-wind farm epibiotic variability should be a priority for future research, improving our understanding of how large OWFs interact with local and regional marine ecosystems.

Data statement

The abundance data set and machine-learning model are available via Figshare at https://figshare.com/s/4b6574449209662f5ba8. Due to the anonymous nature of the data provision, the ROV imagery and 3D models will not be made available.

CRediT authorship contribution statement

Joseph Marlow: Conceptualization, Data curation, Formal analysis, Methodology, Visualization, Writing – original draft. **John E. Halpin:** Data curation, Formal analysis, Methodology, Writing – review & editing. **Thomas A. Wilding:** Funding acquisition, Supervision, Writing – review & editing.

Declaration of competing interest

The authors declare that they have no known competing financial interests or personal relationships that could have appeared to influence the work reported in this paper.

Acknowledgements

The authors would like to thank INSITE/NERC for providing the funding for this research under grant no. NE/T010665/1 and to thank our anonymous industry partners who provided ROV time and ROV imagery. We would also like to thank Sally Rouse for instigating and facilitating our industry collaboration.

Appendix A. Supplementary data

Supplementary data to this article can be found online at https://doi.org/10.1016/j.marenvres.2026.108180.

Data availability

Data link provided in Data Statement.

Quantifying intra-windfarm spatial heterogeneity in epibiotic assemblages using automated image analysis (Original data) (Figshare)

References

Andersson, M.H., Berggren, M., Wilhelmsson, D., Öhman, M.C., 2009. Epibenthic colonization of concrete and steel pilings in a cold-temperate embayment: a field experiment. Helgol. Mar. Res. 63 (3), 3. https://doi.org/10.1007/s10152-009-0156-9.

Angiolillo, M., Gori, A., Canese, S., Bo, M., Priori, C., Bavestrello, G., Salvati, E., Erra, F., Greenacre, M., Santangelo, G., 2016. Distribution and population structure of deep-dwelling red coral in the northwest mediterranean. Mar. Ecol. 37 (2), 294–310. https://doi.org/10.1111/maec.12274.

Bayley, B., Griffiths, T., Pistani, F., Helmholz, P., Belton, D., Parnum, I., 2024. Quantifying marine growth on pipelines with archival remotely operated vehicle footage – a case study. ISPRS Ann. Photogr. Rem. Sens. Spat. Inform. Sci. X-4–2024, 45–50. https://doi.org/10.5194/isprs-annals-X-4-2024-45-2024.

Bishop, M.J., Mayer-Pinto, M., Airoldi, L., Firth, L.B., Morris, R.L., Loke, L.H.L., Hawkins, S.J., Naylor, L.A., Coleman, R.A., Chee, S.Y., Dafforn, K.A., 2017. Effects of ocean sprawl on ecological connectivity: impacts and solutions. J. Exp. Mar. Biol. Ecol. 492, 7–30. https://doi.org/10.1016/j.jembe.2017.01.021.

Bull, A.S., Love, M.S., 2019. Worldwide oil and gas platform decommissioning: a review of practices and reefing options. Ocean Coast Manag. 168, 274–306. https://doi.org/10.1016/j.ocecoaman.2018.10.024.

Burdon, D., Boyes, S.J., Elliott, M., Smyth, K., Atkins, J.P., Barnes, R.A., Wurzel, R.K., 2018. Integrating natural and social sciences to manage sustainably vectors of change in the marine environment: Dogger Bank transnational case study. Estuar. Coast. Shelf Sci. Vect. Chang. Mar. Environ. 201, 234–247. https://doi.org/10.1016/j.ecss.2015.09.012.

Christiansen, N., Carpenter, J.R., Daewel, U., Suzuki, N., Schrum, C., 2023. The large-scale impact of anthropogenic mixing by offshore wind turbine foundations in the shallow north sea. Front. Mar. Sci. 10, 1178330. https://doi.org/10.3389/fmars.2023.1178330.

Coates, D.A., Deschutter, Y., Vincx, M., Vanaverbeke, J., 2014. Enrichment and shifts in macrobenthic assemblages in an offshore wind farm area in the Belgian part of the north sea. Mar. Environ. Res. 95, 1–12. https://doi.org/10.1016/j.marenvres.2013.12.008.

Coolen, J.W.P., Boon, A.R., Crooijmans, R., van Pelt, H., Kleissen, F., Gerla, D., Beermann, J., Birchenough, S.N.R., Becking, L.E., Luttikhuizen, P.C., 2020a. Marine stepping-stones: connectivity of Mytilus edulis populations between offshore energy installations. Mol. Ecol. 29 (4), 686–703. https://doi.org/10.1111/mec.15364.

Coolen, J.W.P., Van Der Weide, B., Cuperus, J., Blomberg, M., Van Moorsel, G.W.N.M., Faasse, M.A., Bos, O.G., Degraer, S., Lindeboom, H.J., 2020b. Benthic biodiversity on old platforms, young wind farms, and rocky reefs. ICES (Int. Counc. Explor. Sea) J. Mar. Sci. 77 (3), 1250–1265. https://doi.org/10.1093/icesjms/fsy092.

Daewel, U., Akhtar, N., Christiansen, N., Schrum, C., 2022. Offshore wind farms are projected to impact primary production and bottom water deoxygenation in the North Sea. Commun. Earth Environ. 3 (1), 292. https://doi.org/10.1038/s43247-022-00625-0.

De Mesel, I., Kerckhof, F., Norro, A., Rumes, B., Degraer, S., 2015. Succession and seasonal dynamics of the epifauna community on offshore wind farm foundations

and their role as stepping stones for non-indigenous species. Hydrobiologia 756. https://doi.org/10.1007/s10750-014-2157-1.
Dorrell, R.M., Lloyd, C.J., Lincoln, B.J., Rippeth, T.P., Taylor, J.R., et al., 2022. Anthropogenic mixing in seasonally stratified shelf seas by offshore wind farm infrastructure. Front. mar. sci. 9, 830927. https://doi.org/10.3389/fmars.2022.830927. https://www.frontiersin.org/articles/10.3389/fmars.2022.830927/full. (Accessed 22 March 2022).
Duarte, C.M., Pitt, K.A., Lucas, C.H., Purcell, J.E., Uye, S., Robinson, K., Brotz, L., Decker, M.B., Sutherland, K.R., Malej, A., Madin, L., Mianzan, H., Gili, J.-M., Fuentes, V., Atienza, D., Pagés, F., Breitburg, D., Malek, J., Graham, W.M., Condon, R.H., 2013. Is global ocean sprawl a cause of jellyfish blooms? Front. Ecol. Environ. 11 (2), 91–97. https://doi.org/10.1890/110246.
Dubois, A., Schoefs, F., Cognie, B., Reynaud, M., Soulard, T., Dumay, J., 2025. Spatio-temporal evolution and engineering implications of biofouling communities on floating wind turbines mooring lines. Estuar. Coast Shelf Sci. 320, 109302. https://doi.org/10.1016/j.ecss.2025.109302.
Firth, W.L.B., Knights, A.M., Bridger, D., Evans, A.J., Mieszkowska, N., Moore, P.J., O'Connor, N.E., Sheehan, E.V., Hawkins, R.C.T.&S.J., 2016. Ocean sprawl: challenges and opportunities for biodiversity management in a changing world. In: Oceanography and Marine Biology. CRC Press.
Floeter, J., Van Beusekom, J.E.E., Auch, D., Callies, U., Carpenter, J., Dudeck, T., Eberle, S., Eckhardt, A., Gloe, D., Hänselmann, K., Hufnagl, M., Janßen, S., Lenhart, H., Möller, K.O., North, R.P., Pohlmann, T., Riethmüller, R., Schulz, S., Spreizenbarth, S., et al., 2017. Pelagic effects of offshore wind farm foundations in the stratified North Sea. Prog. Oceanogr. 156, 154–173. https://doi.org/10.1016/j.pocean.2017.07.003.
Forteath, G., Picken, G., Ralph, R., Williams, J., 1982. Marine growth studies on the North Sea oil platform montrose alpha. Mar. Ecol. Prog. Ser. 8, 61–68. https://doi.org/10.3354/meps008061.
Friedlander, A.M., Ballesteros, E., Fay, M., Sala, E., 2014. Marine communities on oil platforms in Gabon, West Africa: high biodiversity oases in a low biodiversity environment. PLoS One 9 (8), e103709. https://doi.org/10.1371/journal.pone.0103709.
Gass, S.E., Roberts, J.M., 2006. The occurrence of the cold-water coral Lophelia pertusa (Scleractinia) on oil and gas platforms in the North Sea: colony growth, recruitment and environmental controls on distribution. Mar. Pollut. Bull. 52 (5), 549–559. https://doi.org/10.1016/j.marpolbul.2005.10.002.
Gormley, K., McLellan, F., McCabe, C., Hinton, C., Ferris, J., Kline, D., Scott, B., 2018. Automated image analysis of offshore infrastructure marine biofouling. J. Mar. Sci. Eng. 6 (1), 2. https://doi.org/10.3390/jmse6010002.
Gourvenec, S., Sturt, F., Reid, E., Trigos, F., 2022. Global assessment of historical, current and forecast ocean energy infrastructure: Implications for marine space planning, sustainable design and end-of-engineered-life management. Renew. Sustain. Energy Rev. 154, 111794. https://doi.org/10.1016/j.rser.2021.111794, 111794. https://linkinghub.elsevier.com/retrieve/pii/S1364032121010637.
Guerin, A.J., 2009. *Marine Communities of North Sea Offshore Platforms, and the Use of Stable Isotopes to Explore Artificial reef Food Webs* [PhD Thesis. University of Southampton. https://eprints.soton.ac.uk/168947/1/Guerin_PhD_2010.pdf.
Harris, C.B., Benjamins, S., Scott, B., Williamson, B.J., 2025. Ecological impacts of floating offshore wind on marine mammals and associated trophic interactions: current evidence and knowledge gaps. Mar. Pollut. Bull. 218, 118059. https://doi.org/10.1016/j.marpolbul.2025.118059.
Hartnoll, R.G., 1975. The annual cycle of *Alcyonium digitatum*. Estuar. Coast Mar. Sci. 3 (1), 71–78. https://doi.org/10.1016/0302-3524(75)90006-7.
Henry, L.-A., Mayorga-Adame, C.G., Fox, A.D., Polton, J.A., Ferris, J.S., McLellan, F., McCabe, C., Kutti, T., Roberts, J.M., 2018. Ocean sprawl facilitates dispersal and connectivity of protected species. Sci. Rep. 8 (1), 11346. https://doi.org/10.1038/s41598-018-29575-4.
Hiscock, K., Sharrock, S., Highfield, J., Snelling, D., 2010. Colonization of an artificial reef in south-west England—Ex-HMS 'Scylla.'. J. Mar. Biol. Assoc. U. K. 90 (1), 69–94. https://doi.org/10.1017/S0025315409991457.
Iakubovskii, P., 2019. Segmentation Models Pytorch. In: In: GitHub repository. GitHub. https://github.com/qubvel/segmentation_models.pytorch.
IRENA 2023: https://www.irena.org/-/media/Files/IRENA/Agency/Publication/2023/Sep/IRENA_GWEC_Enabling_frameworks_offshore_win.
Joschko, T.J., Buck, B.H., Gutow, L., Schröder, A., 2008. Colonization of an artificial hard substrate by *Mytilus edulis* in the German Bight. Mar. Biol. Res. 4 (5), 350–360. https://doi.org/10.1080/17451000801947043.
Karlsson, R., Tivefälth, M., Duranović, I., Martinsson, S., Kjølhamar, A., Murvoll, K.M., 2022. Artificial hard-substrate colonisation in the offshore hywind Scotland pilot park. Wind Energy Sci. 7 (2), 801–814. https://doi.org/10.5194/wes-7-801-2022.
Kerckhof, F., Degraer, S., Norro, A., Rumes, B., 2011. Offshore intertidal hard substrata: a new habitat promoting non-indigenous species in the southern North Sea: an exploratory study, 2011. In: Degraer, S., Brabant, R., Rumes, B. (Eds.), Offshore Wind Farms in the Belgian Part of the North Sea: Selected Findings from the Baseline and Targeted Monitoring. Royal Belgian Institute of Natural Sciences, Management Unit of the North Sea Mathematical Models. Marine ecosystem management unit. 157 pp. + annex. https://odnature.naturalsciences.be/mumm/documents/9/mumm-monitoring-windfarm-2011-en.pdf.
Kerckhof, F., Rumes, B., Degraer, S., 2019. About "Mytilisation" and "Slimeification": a decade of succession of the fouling assemblages on wind turbines off the Belgian coast. In: Degraer, S., Brabant, R., Rumes, B., Vigin, L. (Eds.), Environmental Impacts of Offshore Wind Farms in the Belgian Part of the North Sea: Marking a Decade of Monitoring, Research and Innovation. Brussels: Royal Belgian Institute of Natural Sciences, OD Natural Environment. Marine Ecology and Management, p. 134, 2019. https://odnature.naturalsciences.be/mumm/documents/14/mumm-monitoring-windfarm-2019-en.pdf.
Kerckhof, F., Rumes, B., Jacques, T., Degraer, S., Norro, A., 2010. Early development of the subtidal marine biofouling on a concrete offshore windmill foundation on the Thornton bank (southern North Sea): first monitoring results. Underw. Technol. 29 (3), 137–149. https://doi.org/10.3723/ut.29.137.
Krone, R., Gutow, L., Joschko, T.J., Schröder, A., 2013. Epifauna dynamics at an offshore foundation – implications of future wind power farming in the North Sea. Mar. Environ. Res. 85, 1–12. https://doi.org/10.1016/j.marenvres.2012.12.004.
Langhamer, O., 2010. Colonization of blue mussels (*Mytilus edulis*) on offshore wave power installations. In: Chan, J., Wong, S. (Eds.), Biofouling: Types, Impacts and Anti-fouling. Nova Science Publishers Inc, Hauppauge, NY, pp. 295–308, pp. 295–308.
Le Marchand, M., Ben Rais Lasram, F., Araignous, E., Halouani, G., Bourdaud, P., Safi, G., Niquil, N., Le Loc'h, F., 2025. Towards an ecosystem approach to a simulated floating wind farm combined with climate change in the Bay of Biscay (France). Reg. Stud. Mar. Sci. 87, 104218. https://doi.org/10.1016/j.rsma.2025.104218.
Lefaible, N., Braeckman, U., Degraer, S., Vanaverbeke, J., Moens, T., 2023. A wind of change for soft-sediment infauna within operational offshore windfarms. Mar. Environ. Res. 188, 106009. https://doi.org/10.1016/j.marenvres.2023.106009.
Lemasson, A.J., Somerfield, P.J., Schratzberger, M., Thompson, M.S.A., Firth, L.B., Couce, E., McNeill, C.L., Nunes, J., Pascoe, C., Watson, S.C.L., Knights, A.M., 2024. A global meta-analysis of ecological effects from offshore marine artificial structures. Nat. Sustain. 7 (4), 485–495. https://doi.org/10.1038/s41893-024-01311-z.
Lombardi, M.R., Lesser, M.P., 2010. The annual gametogenic cycle of the sea anemone *Metridium senile* from the Gulf of Maine. J. Exp. Mar. Biol. Ecol. 390 (1), 58–64. https://doi.org/10.1016/j.jembe.2010.04.004.
Maar, M., Bolding, K., Petersen, J.K., Hansen, J.L.S., Timmermann, K., 2009. Local effects of blue mussels around turbine foundations in an ecosystem model of Nysted offshore wind farm, Denmark. J. Sea Res. 62 (2–3), 159–174. https://doi.org/10.1016/j.seares.2009.01.008.
Maksassi, Z., Garnier, B., Moctar, A.O.E., Schoefs, F., Schaeffer, E., 2022. Thermal characterization and thermal effect assessment of biofouling around a dynamic submarine electrical cable. Energies 15 (9), 3087. https://doi.org/10.3390/en15093087.
Maksassi, Z., Moctar, A.O.E., Garnier, B., Schoefs, F., Schaeffer, E., 2024. For better comprehension of mussel's thermal characteristics and their thermal effect on dynamic submarine electrical cables. Appl. Ocean Res. 144, 103900. https://doi.org/10.1016/j.apor.2024.103900.
Marlow, J., Halpin, J.E., Wilding, T.A., 2024. 3D photogrammetry and deep-learning deliver accurate estimates of epibenthic biomass. Methods Ecol. Evol. 15 (5), 965–977. https://doi.org/10.1111/2041-210X.14313.
Martins, G.M., Patarra, R.F., Álvaro, N.V., Prestes, A.C.L., Neto, A.I., 2013. Effects of coastal orientation and depth on the distribution of subtidal benthic assemblages. Mar. Ecol. 34 (3), 289–297. https://doi.org/10.1111/maec.12014.
McCoy, A., Musial, W., Hammond, R., Hernando, D.M., Duffy, P., Beiter, P., Pérez, P., Baranowski, R., Reber, G., Spitsen, P., 2024. Offshore Wind Market Report, Edition (n.d.).
McLean, D.L., Ferreira, L.C., Benthuysen, J.A., Miller, K.J., Schläppy, M.-L., Ajemian, M. J., Berry, O., Birchenough, S.N.R., Bond, T., Boschetti, F., Bull, A.S., Claisse, J.T., Condie, S.A., Consoli, P., Coolen, J.W.P., Elliott, M., Fortune, I.S., Fowler, A.M., Gillanders, B.M., et al., 2022. Influence of offshore oil and gas structures on seascape ecological connectivity. Glob. Change Biol. 28 (11), 3515–3536. https://doi.org/10.1111/gcb.16134.
McLean, D.L., Parsons, M.J.G., Gates, A.R., Benfield, M.C., Bond, T., Booth, D.J., Bunce, M., Fowler, A.M., Harvey, E.S., Macreadie, P.I., Pattiaratchi, C.B., Rouse, S., Partridge, J.C., Thomson, P.G., Todd, V.L.G., Jones, D.O.B., 2020. Enhancing the scientific value of industry remotely operated vehicles (ROVs) in Our oceans. Front. Mar. Sci. 7, 220. https://doi.org/10.3389/fmars.2020.00220.
Molen, J.V.D., García-García, L.M., Whomersley, P., Callaway, A., Posen, P.E., Hyder, K., 2018. Connectivity of larval stages of sedentary marine communities between hard substrates and offshore structures in the North Sea. Sci. Rep. 8 (1), 14772. https://doi.org/10.1038/s41598-018-32912-2.
Nelson, M., Craig, S., 2011. Role of the sea anemone Metridium senile in structuring a developing subtidal fouling community. Mar. Ecol. Prog. Ser. 421, 139–149. https://doi.org/10.3354/meps08838.
Nieradzinska, K., MacIver, C., Gill, S., Agnew, G.A., Anaya-Lara, O., Bell, K.R.W., 2016. Optioneering analysis for connecting Dogger Bank offshore wind farms to the GB electricity network. Renew. Energy 91, 120–129. https://doi.org/10.1016/j.renene.2016.01.043.
Oksanen, J., Simpson, G.L., Blanchet, F.G., Kindt, R., Legendre, P., Minchin, P.R., O'Hara, R.B., Solymos, P., Stevens, M.H.H., Szoecs, E., Wagner, H., Barbour, M., Bedward, M., Bolker, B., Borcard, D., Borman, T., Carvalho, G., Chirico, M., Caceres, M.D., et al., 2025. In: Vegan: Community Ecology Package (Version 2.7-2) [Computer software]. https://cran.r-project.org/web/packages/vegan/index.html.
Oshurkov, V.V., 1992. Succession and climax in some fouling communities. Biofouling 6 (1), 1–12. https://doi.org/10.1080/08927019209386205.
Palma, M., Rivas Casado, M., Pantaleo, U., Pavoni, G., Pica, D., Cerrano, C., 2018. SfM-Based method to assess gorgonian forests (Paramuricea clavata (Cnidaria, Octocorallia)). Remote Sens. 10 (7), 1154. https://doi.org/10.3390/rs10071154.
Perrow, M.R., Gilroy, J.J., Skeate, E.R., Tomlinson, M.L., 2011. Effects of the construction of Scroby Sands offshore wind farm on the prey base of little tern *Sternula albifrons* at its most important UK colony. Mar. Pollut. Bull. 62 (8), 1661–1670. https://doi.org/10.1016/j.marpolbul.2011.06.010.

Petersen, J.K., Nielsen, T.G., Duren, L. van, Maar, M., 2008. Depletion of plankton in a raft culture of Mytilus galloprovincialis in Ría de Vigo, NW Spain. I. Phytoplankton. Aquat. Biol. 4, 113–125. https://doi.org/10.3354/ab00124.

Pierce, J., Butler, M.J., Rzhanov, Y., Lowell, K., Dijkstra, J.A., 2021. Classifying 3-D models of coral reefs using structure-from-motion and multi-view semantic segmentation. Front. Mar. Sci. 8. https://doi.org/10.3389/fmars.2021.706674.

Raoux, A., Lassalle, G., Pezy, J.-P., Tecchio, S., Safi, G., Ernande, B., Mazé, C., Loc'h, F.L., Lequesne, J., Girardin, V., Dauvin, J.-C., Niquil, N., 2019. Measuring sensitivity of two OSPAR indicators for a coastal food web model under offshore wind farm construction. Ecol. Indic. 96, 728–738. https://doi.org/10.1016/j.ecolind.2018.07.014.

Raoux, A., Tecchio, S., Pezy, J.-P., Lassalle, G., Degraer, S., Wilhelmsson, D., Cachera, M., Ernande, B., Le Guen, C., Haraldsson, M., Grangeré, K., Le Loc'h, F., Dauvin, J.-C., Niquil, N., 2017. Benthic and fish aggregation inside an offshore wind farm: which effects on the trophic web functioning? Ecol. Indic. 72, 33–46. https://doi.org/10.1016/j.ecolind.2016.07.037.

Sammarco, P.W., Lirette, A., Tung, Y.F., Boland, G.S., Genazzio, M., Sinclair, J., 2014. Coral communities on artificial reefs in the Gulf of Mexico: standing vs. toppled oil platforms. ICES (Int. Counc. Explor. Sea) J. Mar. Sci. 71 (2), 417–426. https://doi.org/10.1093/icesjms/fst140.

Schultze, L.K.P., Merckelbach, L.M., Horstmann, J., Raasch, S., Carpenter, J.R., 2020. Increased mixing and turbulence in the wake of offshore wind farm foundations. J. Geophys. Res., Oceans 125 (8). https://doi.org/10.1029/2019JC015858 e2019JC015858.

Schutter, M., Dorenbosch, M., Driessen, F.M.F., Lengkeek, W., Bos, O.G., Coolen, J.W.P., 2019. Oil and gas platforms as artificial substrates for epibenthic North Sea fauna: effects of location and depth. J. Sea Res. 153, 101782. https://doi.org/10.1016/j.seares.2019.101782.

Sebens, K.P., Koehl, M.A.R., 1984. Predation on zooplankton by the benthic anthozoans Alcyonium siderium (Alcyonacea) and Metridium senile (Actiniaria) in the New England subtidal. Mar. Biol. 81 (3), 255–271. https://doi.org/10.1007/bf00393220. http://link.springer.com/10.1007/BF00393220.

Sharma, P., Bisht, I., Sur, A., 2023. Wavelength-based attributed deep neural network for underwater image restoration. ACM Trans. Multimedia Comput. Commun. Appl. 19 (1). https://doi.org/10.1145/3511021, 2:1-2:23.

Signor, J., Schoefs, F., Quillien, N., Damblans, G., 2023. Automatic classification of biofouling images from offshore renewable energy structures using deep learning. Ocean Eng. 288, 115928. https://doi.org/10.1016/j.oceaneng.2023.115928.

Slavik, K., Lemmen, C., Zhang, W., Kerimoglu, O., Klingbeil, K., Wirtz, K.W., 2019. The large-scale impact of offshore wind farm structures on pelagic primary productivity in the southern North Sea. Hydrobiologia 845 (1), 35–53. https://doi.org/10.1007/s10750-018-3653-5.

Spielmann, V., Dannheim, J., Brey, T., Coolen, J.W.P., 2023. Decommissioning of offshore wind farms and its impact on benthic ecology. J. Environ. Manag. 347, 119022. https://doi.org/10.1016/j.jenvman.2023.119022.

Spyksma, A.J.P., Miller, K.I., Shears, N.T., 2022. Diver-generated photomosaics as a tool for monitoring temperate rocky reef ecosystems. Front. Mar. Sci. 9, 953191. https://doi.org/10.3389/fmars.2022.953191.

Squire, M., Madgett, A., Burdon, D., Scott, B., Marlow, J., Gormley, K., 2026. Understanding the role of offshore energy structures in ecosystem service delivery: applying global findings to the North Sea. Ecosyst. Serv. 78, 101811. https://doi.org/10.1016/j.ecoser.2025.101811.

Stamp, T., Tyler-Walters, H., Lloyd, K., Watson, A., 2023. Tubularia indivisa on tide-swept circalittoral rock. In: Marine Life Information Network: Biology and Sensitivity Key Information Reviews. Marine Biological Association of the United Kingdom, Plymouth.

Sullivan, C.B., Kaszynski, A.A., 2019. PyVista: 3D plotting and mesh analysis through a streamlined interface for the Visualization Toolkit (VTK). J. Open Source Softw. 4 (37), 1450. https://doi.org/10.21105/joss.01450.

Sutherland, J.P., 1974. Multiple stable points in natural communities. Am. Nat. 108 (964), 859–873.

Thomson, P.G., Fowler, A.M., Davis, A.R., Pattiaratchi, C.B., Booth, D.J., 2018. Some old movies become classics – a case Study determining the scientific value of ROV inspection footage on a platform on Australia's North West Shelf. Front. Mar. Sci. 5, 471. https://doi.org/10.3389/fmars.2018.00471.

Todd, V.L.G., Susini, I., Williamson, L.D., Todd, I.B., McLean, D.L., Macreadie, P.I., 2021. Characterizing the second wave of fish and invertebrate colonization of an offshore petroleum platform. ICES (Int. Counc. Explor. Sea) J. Mar. Sci. 78 (3), 1131–1145. https://doi.org/10.1093/icesjms/fsaa245.

Todd, V.L.G., Williamson, L.D., Cox, S.E., Todd, I.B., Macreadie, P.I., 2020. Characterizing the first wave of fish and invertebrate colonization on a new offshore petroleum platform. ICES (Int. Counc. Explor. Sea) J. Mar. Sci. 77 (3), 1127–1136. https://doi.org/10.1093/icesjms/fsz077.

Van Der Stap, T., Coolen, J.W.P., Lindeboom, H.J., 2016. Marine fouling assemblages on offshore gas platforms in the southern North Sea: effects of depth and distance from shore on biodiversity. PLoS One 11 (1), e0146324. https://doi.org/10.1371/journal.pone.0146324.

Want, A., Crawford, R., Kakkonen, J., Kiddie, G., Miller, S., Harris, R.E., Porter, J.S., 2017. Biodiversity characterisation and hydrodynamic consequences of marine fouling communities on marine renewable energy infrastructure in the Orkney Islands Archipelago, Scotland, UK. Biofouling 33 (7), 567–579. https://doi.org/10.1080/08927014.2017.1336229.

Whomersley, P., Picken, G.B., 2003. Long-term dynamics of fouling communities found on offshore installations in the North Sea. J. Mar. Biol. Assoc. U. K. 83 (5), 897–901. https://doi.org/10.1017/S0025315403008014h.

Wilhelmsson, D., Malm, T., 2008. Fouling assemblages on offshore wind power plants and adjacent substrata. Estuar. Coast Shelf Sci. 79 (3), 459–466. https://doi.org/10.1016/j.ecss.2008.04.020.

Xie, E., Wang, W., Yu, Z., Anandkumar, A., Alvarez, J.M., Luo, P., 2021. SegFormer: Simple and efficient design for semantic segmentation with transformers. Adv. Neural Inf. Process. Syst. 34, 12077–12090.

Zintzen, V., Norro, A., Massin, C., Mallefet, J., 2008a. Spatial variability of epifaunal communities from artificial habitat: shipwrecks in the Southern bight of the North Sea. Estuar. Coast Shelf Sci. 76 (2), 327–344. https://doi.org/10.1016/j.ecss.2007.07.012.

Zintzen, V., Norro, A., Massin, C., Mallefet, J., 2008b. Temporal variation of Tubularia indivisa (Cnidaria, Tubulariidae) and associated epizoites on artificial habitat communities in the North Sea. Mar. Biol. 153 (3), 405–420. https://doi.org/10.1007/s00227-007-0819-5.

Zupan, M., Rumes, B., Vanaverbeke, J., Degraer, S., Kerckhof, F., 2023. Long-term succession on offshore wind farms and the role of species interactions. Diversity 15 (2), 288. https://doi.org/10.3390/d15020288.